Aggregation of LHCII Leads to a Redistribution of the Triplets over the Central Xanthophylls in LHCII

Stefania S. Lampoura,[‡] Virginijus Barzda,[‡,#] Gabrielle M. Owen,[§] Arnold J. Hoff,[§,⊥] and Herbert van Amerongen*,[‡]

Vrije Universiteit, Faculty of Sciences, Division of Physics and Astronomy, Department of Biophysics and Physics of Complex Systems, De Boelelaan 1081, 1081 HV Amsterdam, The Netherlands, and RijksUniversiteit Leiden, Department of Biophysics, Huygens Laboratory, P.O. Box 9504, 2300 RA Leiden, The Netherlands

ABSTRACT: We present laser flash-induced triplet-minus-singlet (TmS_{flash}) and absorbance-detected-magnetic-resonance (TmS_{ADMR}) measurements on the light-harvesting chlorophyll *a/b* pigment−protein complex (LHCII) from pea. We investigated the influence of LHCII aggregation on xanthophyll triplet formation. The effect of aggregation was previously studied using TmS_{ADMR} [van der Vos et al. (1994) *Biochim. Biophys. Acta 1208*, 243−250] for LHCII from spinach, and it was concluded that aggregation leads to a large increase of the amount of intertrimer triplet transfer. However, a similar study on LHCII from pea with the use of TmS_{flash} measurements [Barzda et al. (1998) *Biochemistry 37*, 546−561] showed much smaller effects. To resolve this apparent discrepancy and to compare the results of TmS_{ADMR} and TmS_{flash} measurements, we used both techniques to study LHCII from pea, applying an identical aggregation procedure in both cases. It appears that aggregation does not lead to an increase of intertrimer triplet transfer as thought before but to a redistribution of the triplets over the two central xanthophylls (mainly lutein) that are present in each monomeric subunit of LHCII. Moreover, it is argued that the TmS band at 525 nm is due to lutein instead of violaxanthin as was reported in earlier studies. It is concluded that aggregation leads to a change in chlorophyll−xanthophyll interactions, which might explain the large change in excited-state lifetime of chlorophyll *a* in LHCII upon aggregation. This change in lifetime is possibly related to the phenomenon of nonphotochemical quenching in green plants, which is an important protective regulatory mechanism, that lowers the probability of photoinhibition.

The utilization of absorbed sunlight energy in photosynthetic organisms proceeds via singlet excited states of the chromophores (chlorophyll (Chl)[1] and carotenoid (Car)) (*1*, *2*). Excitation energy is transported from the light-harvesting complexes to the reaction center where it leads to a charge separation, which ultimately leads to the production of chemical energy. However, a small fraction of the excitations ends up in Chl triplet states (*3*), which represent not only an energy loss channel, but are also potentially dangerous for the living organisms due to their high reactivity with oxygen, leading to the formation of the very reactive singlet oxygen molecules. Photosynthetic organisms utilize Cars to protect the system from singlet oxygen production.

Car and Chl triplets in light-harvesting Chl *a/b* pigment−protein complex (LHCII) of photosystem II of green plants have been examined in the past by electron paramagnetic resonance (EPR) (*4*), laser-flash triplet-minus-singlet (TmS_{flash}) (*5−10*), and optically detected magnetic resonance (ODMR) measurements (*11*, *12*), and different Car triplets were distinguished. Moreover, both TmS_{flash} and absorbance-detected magnetic resonance (ADMR) measurements revealed spectral changes in the Chl region upon triplet formation on the Cars, due to strong interactions between both types of chromophores (*5*, *8*, *11*). Spectrally different Cars appeared to be in contact with Chls that are also spectroscopically distinguishable, although the specific molecules could not be identified at that time (*5*, *11*).

Three different carotenoids, namely, lutein, violaxanthin, and neoxanthin, coexist in trimeric LHCII (*3*), which is the most abundant antenna complex of green plants. These carotenoids are termed xanthophylls because they contain oxygen functions. The 3.4 Å crystallographic structure revealed by electron diffraction on 2D crystals (*13*) shows two luteins in the center of each LHCII monomer. The approximate location and orientation of a third xanthophyll, namely, neoxanthin, were resolved by Croce et al. (*14*). The luteins are predominantly in contact with Chl *a* molecules, and excitation of luteins in trimeric LHCII is followed by rapid excitation energy transfer to mainly Chl a (*15*, *16*),

---

* Corresponding author: tel.: +31-20-4447931; fax.: +31-20-4447999; e-mail: herbert@nat.vu.nl.

‡ Vrije Universiteit.

§ RijksUniversiteit Leiden.

Present address: Department of Chemistry and Biochemistry, University of California, San Diego, 9500 Gilman Drive, La Jolla, CA 92093, U.S.A.

⊥ Deceased.

[1] Abbreviations: ADMR, absorbance-detected magnetic resonance; Car, carotenoid; CD, circular dichroism; Chl, chlorophyll; CMC, critical micelle concentration; DAS, decay-associated spectrum; DM, *n*-dodecyl β-D-maltoside; EPR, electron paramagnetic resonance; FDMR, fluorescence-detected magnetic resonance; LHCII, light-harvesting complex II from green plants; ODMR, optically detected magnetic resonance; TmS, triplet-minus-singlet; TmS_{flash}, flash-induced triplet-minus-singlet; TmS_{ADMR}, triplet-minus-singlet, detected via ADMR.

whereas the neoxanthin is located next to at least two Chl *b* molecules (*14*). A fourth xanthophyll, namely, violaxanthin, is easily lost upon isolation (*17*); it is located at the outside of the complex, and it does not transfer excitation energy toward the Chls (*18*). Usually, violaxanthin is found in substoichiometric amounts, i.e., there is less than one molecule per LHCII monomer after isolation. It is generally agreed upon that the lowest energy absorption maximum of neoxanthin is located near 487 nm (*6, 19*). Flash-induced TmS measurements did not reveal any triplet transfer from Chls to this neoxanthin molecule, and therefore the amount of transfer should be small (*5−7*). This is understandable because singlet excitation energy transfer from Chl *b* to Chl *a* is very fast (*20*) and triplets are mainly formed on Chl *a* molecules, which are lower in energy than the Chl *b* molecules, whereas the latter are presumably the "neighbors" of the neoxanthin.

TmS measurements showed strong absorption bands of xanthophyll triplets with maxima at approximately 507 and 525 nm (*5−12*). It was demonstrated for LHCII trimers that the 525 nm triplet absorption band corresponds to a xanthophyll with a weak singlet absorption band at 510 nm (*6*). Upon monomerization of LHCII both the 510 nm singlet absorption and the 525 nm triplet absorption band disappear (*6*). The 507 nm triplet band corresponds to a relatively strong 494 nm singlet absorption band (*6*). Assuming that both luteins absorb at the same wavelength, the strong 494 nm band was assigned to lutein and the weak 510 nm band to violaxanthin (*6*). The observation that monomerization of LHCII led to a substantial loss of violaxanthin molecules, concomitant with the loss of the 510 nm singlet and 525 nm triplet absorption bands, was taken as additional support for this assignment (*6*) (but see below).

An important feature of LHCII is its ability to form large aggregates. The aggregation state of LHCII is strongly dependent on protein and detergent concentrations in the suspension (*21−23*). It was observed by ADMR and fluorescence-detected-magnetic resonance (FDMR) that the ratio of the Car triplet signals at 507 and 525 nm is strongly dependent on the LHCII concentration and thus the amount of aggregation (*12, 24*); however, this was only true when tuning to the |D| + |E| transition around 1300 MHz, while the spectrum obtained when exciting the 2|E| transition was not affected. The strong relative increase of the 525 nm band upon aggregation was ascribed to increased intertrimer triplet transfer. A room temperature TmS$_{flash}$ study on LHCII from pea did not show a clear band at 525 nm, but aggregation led to a broadening of the main TmS band near 507 nm toward the red, consistent with the low-temperature experiments (*8*). Another TmS$_{flash}$ study on LHCII from pea also showed a relative increase of the 525 nm band, both at room temperature and cryogenic temperatures, but the effect was far less pronounced (*7*). A similar explanation was given for this increase, i.e., intertrimer triplet transfer, and the peripheral location of the violaxanthin molecule and its presumed triplet absorption maximum around 525 nm strongly suggested an increased triplet transfer from Chl to violaxanthin upon aggregation. However, the difference in the size of the effect in the two studies (*7, 12*) remained unexplained. Several explanations are possible: (i) different starting material for LHCII preparation, i.e., spinach (*12*) vs pea (*7*); (ii) different techniques; (iii) different methods of aggregation, i.e., variation of the LHCII concentration (*12*) vs variation of the detergent concentration (*7*). To resolve this problem, we have now performed both TmS$_{flash}$ and TmS$_{ADMR}$ measurements on the same preparation, i.e., LHCII from pea, which was aggretated by changing the detergent concentration. Moreover, a similar temperature was used in both experiments, i.e., 1.2 K for TmS$_{ADMR}$ and 5 K for TmS$_{flash}$.

A comparison of the apparently controversial results as indicated above has gained importance in light of several recent publications on LHCII. It was found by Ruban and co-workers (*25, 26*) that the 510 nm singlet absorption band should not be ascribed to violaxanthin but to lutein. The latter has an absorption maximum below 500 nm in monomeric LHCII, which shifts to 510 nm upon trimerization. This was confirmed by Bassi and co-workers who found that a small fraction of the lutein molecules has an absorption maximum near 510 nm in trimeric LHCII (*18*). This disqualifies the explanation given above that upon aggregation the peripheral violaxanthin accepts relatively more triplets, suggesting that the spectral changes must be explained by changes in the chlorophyll−carotenoid interactions. In principle, this could be an important issue because such a change in interaction might lead to a change in the excited-state lifetime of the chlorophylls in LHCII (*27−29*), which might offer at least a partial explanation for the important regulatory mechanism in green plants, called nonphotochemical quenching (see below). The latter process provides plants with the possibility to adapt to strong light conditions, thereby significantly decreasing the amount of photoinhibition (see, e.g., ref *30*). Despite huge research efforts, a physical explanation for this process has not been found yet.

MATERIALS AND METHODS

Stacked lamellar aggregates of LHCII were isolated from leaves of 2-week-old pea (*Pisum* sativum) plants as described in ref *23*. LHCII was stored in a 15 mM Tricine/NaOH, pH 7.8 buffer at 4 °C and used within two weeks after isolation. These samples were used, both for low-temperature TmS$_{ADMR}$ and TmS$_{flash}$ measurements. The pigment composition was determined by high-pressure-liquid-chromatography (HPLC) analysis and resulted in the ratio 7.2:6:1.8:0.6:0.3 for Chl *a*, Chl *b*, lutein, neoxanthin, and violaxanthin, respectively.

For disaggregation of LHCII aggregates, *n*-dodecyl β-D-maltoside (DM) was used. The state of aggregation was monitored by circular-dichroism (CD) and fluorescence measurements as described in refs *21* and *31*. The critical micelle concentration (CMC, the concentration at which LHCII aggregates are disassembled into trimers) of DM for this type of LHCII preparation was about 0.009% (w/v).

Low-temperature measurements were performed in a helium bath cryostat (Utreks). For the low-temperature TmS$_{flash}$ measurements, the state of aggregation was adjusted by first adding the detergent and then diluting the sample with glycerol, containing the same amount of detergent. The sample was suspended in a mixture of 1/3 buffer + 2/3 glycerol (volume).

Laser-flash-induced triplet-minus-singlet TmS$_{flash}$ absorption difference measurements were performed on the setup described earlier (*32*). Excitation pulses of 8 ns (full width at half-maximum), 590 nm, 10 mJ were provided by a dye

laser (Quanta Ray PDL2, dye: Rhodamine 6G), which was pumped by a frequency-doubled Q-switched Nd:YAG laser (Quanta Ray DCR2). The 20 ms pulses of measuring light were obtained from a 450 W xenon lamp in combination with a shutter. The measuring light was filtered with a set of filters, providing the appropriate wavelength for the measuring beam and minimizing heating and actinic effects. Detection was done via a 1/4 m monochromator and photomultiplier (Hamamatsu R928). The repetition rate of the setup was 2 Hz, and the instrumental response time was less than 0.5 μs. Kinetic traces were averaged 128 or 256 times on a digital oscilloscope, preceding the transfer to the computer for data analysis. TmS$_{flash}$ spectra were constructed from global analysis of the decay kinetics recorded at different wavelengths (*33*). A three exponential model was used for the TmS$_{flash}$ 5 K measurements (see also ref *5*). TmS$_{ADMR}$ measurements were performed at 1.2 K with the setup described in ref *11*. The method is based on the fact that the three triplet sublevels can be populated and depopulated with different rates, leading to different relative population probabilities. In that case, transitions between these sublevels can be induced with the use of microwaves, whereas the transition energies are commonly referred to as $2|E|$, $|D| + |E|$ and $|D| - |E|$. Upon tuning to a particular transition frequency, changes in the absorption spectrum can be monitored, leading to the presented ADMR spectra.

RESULTS

TmS$_{flash}$ Measurements. Global analysis of the TmS$_{flash}$ kinetics at 5 K recorded at different wavelengths revealed three decay-associated spectral components (DAS) in all cases: two Car-associated components with lifetimes of about 5 and 30 μs, and a small Chl component with a lifetime in the millisecond range. TmS$_{flash}$ kinetics was recorded up to 100 μs; thus, the lifetime of the Chl component was not accurately resolved, but here we focus on the Car triplets. The two Car DAS components for LHCII trimers are shown in Figure 1a,b. The 5 μs component has a higher amplitude than the 30 μs one. Both Car DAS reveal two well-characterized peaks at 506 and 525 nm corresponding to different xanthophylls, but their relative size is somewhat different. The different lifetimes occur because at this temperature exchange of population between the three triplet sublevels per xanthophyll is slow or absent. Different sublevels may correspond to different lifetimes. The spectra are similar as in previous measurements on LHCII from spinach and pea (*5, 7*).

The DAS were fitted with two Gaussians, peaking at 506 and 525 nm (Figure 1a), and the areas covered by these two Gaussians were estimated. Representative double Gaussian fits (same peak positions) are also shown in Figure 1b. Both Car DAS components were summed and this sum roughly scales with the total amount of triplets residing on the different xanthophylls after triplet transfer from Chl to Car is complete and before the Car triplet states have started to decay. The ratio of the areas of the 506 and 525 nm bands for the summed spectrum is presented in Figure 1c (circles). The ratios of the 506 and 525 nm bands for the 5 and 30 μs DAS are also shown in the same figure. Aggregation of LHCII was varied by changing the detergent concentration. It is clear from Figure 1c that disaggregation leads to a relative decrease in intensity of the 525 nm band: The ratio
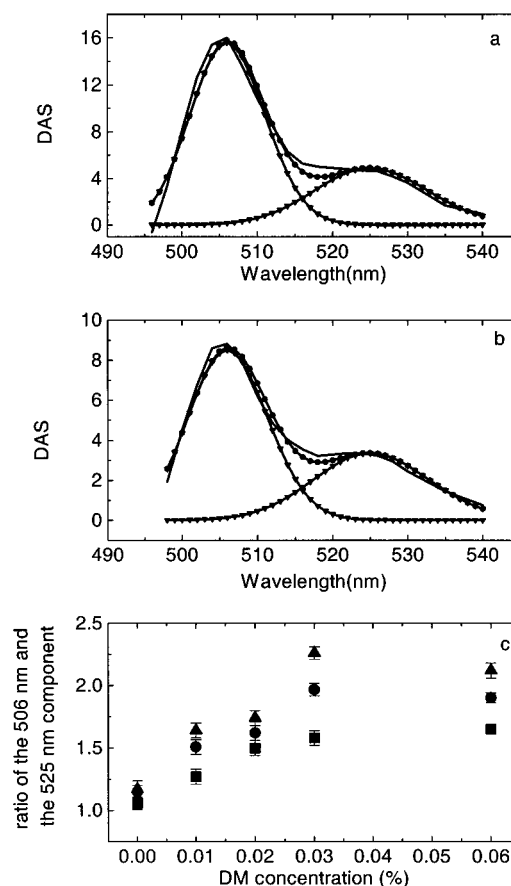

FIGURE 1: (a) A typical double Gaussian fit of the 5 K T-S$_{flash}$ decay associated spectrum of the 5 μs Car component of LHCII trimers. The DM concentration was 0.06%. (b) A typical double Gaussian fit of the 5 K T-S$_{flash}$ decay associated spectrum of the 30 μs Car component of LHCII trimers. The DM concentration was 0.06%. (c) Ratio of the 506 and 525 nm components of the 5 K 5 μs T-S$_{flash}$ decay-associated spectra (squares), the 30 μs decay associated spectra (triangles), and the sum of the 5 and 30 μs decay associated spectra (circles). The aggregation state was controlled by changing the detergent concentration.

of the 506 and 525 nm bands changes from 1.2 for aggregates to 1.9 for trimers. This change is at first sight larger than reported previously (*7*), but it is entirely due to the method of analysis, i.e., comparing areas of fitted Gaussians instead of absorption values at individual wavelengths (506 and 525 nm). However, the variation is significantly smaller than in previous TmS$_{ADMR}$ measurements on LHCII from spinach (0.45 for aggregates and 1 for trimers), where the transition frequency was tuned to the $|D| + |E|$ transition, and the data were also analyzed using Gaussian fits. It should be noted that the transition frequencies are not the same for all xanthophylls involved (*11*), and some selectivity occurs at the used frequency of 1300 MHz. On the other hand, no changes were observed at the $2|E|$ transition, which is very similar for the relevant xanthophylls (*11*). Additional information about the relative population of different Car triplet sublevels can be obtained from TmS$_{ADMR}$ measurements.

TmS$_{ADMR}$ Measurements. The TmS$_{ADMR}$ spectrum of LHCII trimers recorded at the $2|E|$ transition (229 MHz) at 1.2 K is shown in Figure 2a. The TmS$_{ADMR}$ spectra were recorded at different detergent concentrations. In both the previous (*11, 24*) and the current TmS$_{ADMR}$ study, the $2|E|$ transition proves to be the strongest one. All TmS$_{ADMR}$ spectra for
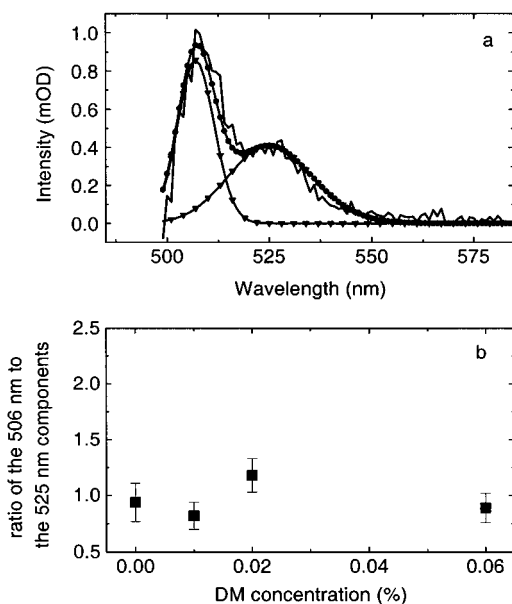
FIGURE 2: (a) T-S$_{ADMR}$ spectrum of LHCII trimers at the 2|E| transition at 229 MHz at 1.2 K, together with a double Gaussian fit. The DM concentration was 0.06%. (b) Ratio of the 506 and 525 nm component of the T-S$_{ADMR}$ at different states of aggregation. The aggregation state was controlled by changing the DM concentration.
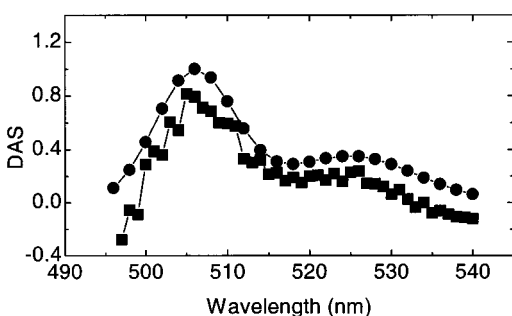

FIGURE 3: 1.2 K T-S$_{ADMR}$ (squares) 2|E| spectrum (Figure 2a) and T-S$_{flash}$ (circles) spectrum of LHCII at 0.06% DM concentration.

different detergent concentrations were fitted with two Gaussians at 507 and 525 nm. Figure 2a illustrates a typical double Gaussian fit of the TmS$_{ADMR}$ spectrum for LHCII trimers with Gaussians centered at 507 and 525 nm. In Figure 2b, the ratio of the 507 and 525 nm components (ratio of band areas) is shown as a function of detergent concentration. From Figure 2b, it is obvious that the aggregation does not influence the ratio of the two components for the 2|E| transition, in agreement with previous studies on LHCII trimers from spinach (*11*). Apparently, the relative increase of the 525 nm component in the TmS$_{flash}$ spectra is not accompanied by a concomitant increase in the 2|E| transition.

In Figure 3, the 5 μs DAS of the TmS$_{flash}$ measurement and the TmS$_{ADMR}$ spectrum (2|E|, 229 MHz), both for 0.06% DM (trimers), are depicted. It is clear that they are very similar, indicating that the TmS$_{ADMR}$ and TmS$_{flash}$ techniques probe the same Cars, in agreement with the fact that all Cars have similar 2|E| transition frequencies (*11*).

Much smaller signals were obtained at the |D| + |E| transition at 1257 MHz, in agreement with previous studies on LHCII from spinach (*11, 12*). The TmS$_{ADMR}$ spectra of
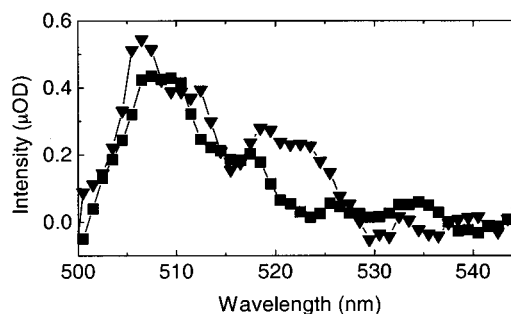

FIGURE 4: T-S$_{ADMR}$ spectrum of LHCII at 0.01% (triangles) and 0.06% DM concentration (squares) probed at the |D| + |E| transition.

LHCII at two different concentrations of 0.01% (aggregates) and 0.06% (trimers) DM are presented in Figure 4. The signal-to-noise ratio is too small to permit a meaningful analysis of the components with a Gaussian fit. However, there is a clear dependence on the detergent concentration, although smaller than in a previous TmS$_{ADMR}$ study on LHCII from spinach (*12*) where the ratio changed from 0.45 to 1 upon changing the amount of aggregation. In the present measurements, the same conditions, both for TmS$_{ADMR}$ and TmS$_{flash}$ experiments were used, and the optical density of the sample was lower than before (*12*).

Like before (*11*), the signals of the |D| − |E| transition were even smaller, and it was impossible to resolve the 507 and 525 components in the present case.

DISCUSSION

Comparison of the Different Results and Techniques. The TmS$_{ADMR}$ results for LHCII from pea (this study) and spinach (*12*) show overall resemblance. Like before, triplet absorption bands are observed at 507 and 525 nm. The size of the absorption difference spectra decreases when tuning from the 2|E|, via the |D| + |E| to the |D| − |E| transition. The ratio of the 2|E| 507 and 525 nm bands is independent of the degree of aggregation, whereas this ratio decreases upon aggregation when tuning to the |D| + |E| transition.

However, there are also differences, and, for instance, the aggregation-dependent decrease in the ratio when tuning to the |D| + |E| transition is smaller than observed before. Moreover, the spectral shape of the absorption difference spectrum is different for trimers from spinach (*11, 12*) and pea when probing the 2|E| transition. Previously, the 525 nm band was larger than or equal to the 507 nm band, and the spectral shape was different from the TmS$_{flash}$ spectrum for spinach trimers (*5*). Now, the 2|E| spectrum resembles the TmS$_{flash}$ spectrum (for pea trimers) which in turn is very similar to the spinach trimer TmS$_{flash}$ spectrum. Therefore, both for spinach and pea trimers, the triplets are similarly distributed over the spectrally different Cars, but the triplets are differently distributed over the triplet sublevels, since the 2|E| spectra differ. Also, the |D| + |E| spectra indicate differences in the pea and spinach preparations. Whereas previously the ratio of the 507 and 525 nm bands changed largely upon changing the degree of aggregation, the effect is now much less pronounced.

Structural Assignment of TmS Bands to Central Xantho-phylls. The change in the ratio of the 507 and 525 nm bands was originally attributed to increased intertrimer triplet

transfer (*12*), and the results in refs *7* and *8* also seemed to be in agreement with this explanation. However, when using this explanation one tacitly assumes that the 507 nm and/or the 525 nm band is/are due to a peripheral xanthophyll as mentioned above. Because the luteins are located in the center of the complex (*13*, *19*, *34*) and the neoxanthin is not responsible for either the 507 or the 525 nm band (see above) only the violaxanthin could in principle be responsible for this effect. However, it was shown by Bassi and co-workers (*18*) that the peripheral violaxanthin does not even transfer singlet excitations to the Chls, thereby excluding the possibility that the peripheral violaxanthin is in van der Waals contact with Chl, a prerequisite for triplet transfer. We therefore conclude that the 507 and 525 nm bands are due to the xanthophylls bound in the center of each monomeric subunit of LHCII at sites L1 and L2 (notation as in ref *35*). Site L1 is exclusively occupied by lutein, whereas site L2 can both bind lutein and violaxanthin with a probability ratio of 0.8:0.2 (*35*), at least in reconstituted LHCII. It was concluded by Peterman et al. (*5*) that three xanthophylls contribute to the TmS spectrum, which is in line with the occupation probability of sites L1 and L2 and the fact that these are responsible for Chl triplet quenching.

We are now in the position to assign the 507 and 525 nm triplet absorption bands. It was shown by Van der Vos et al. (*11*) and Peterman et al. (*5*) with different methods that the xanthophyll responsible for the 525 nm band is in close contact with Chls *a* that absorb more to the blue than those that are in contact with the 507 nm xanthophyll. The xanthophyll at site L1 is in contact with Chls a1, a2, and a3 (for nomenclature see ref *13*) and the one at site L2 with Chls a4–a7. It was concluded that the former on average absorb more to the red (*27*, *36*), and thus it appears that the lutein at site L1 is responsible for the 507 nm triplet band, which corresponds to the 494 nm singlet band (*6*). Consequently, the 525 nm triplet band and thus the 510 nm singlet band (*6*) are due to the lutein at site L2. It should be noted that this site binds a violaxanthin in 20% of the cases whose singlet absorption maximum is close to 494 nm (*6*). Therefore, it seems likely that a triplet on this violaxanthin leads to a triplet absorption band close to 507 nm (presumably like the lutein at L1). By using a simple stoichiometry argument, one thus expects the 507 nm triplet band to be more intense than the 525 nm triplet band, in agreement with experimental findings. In addition, the lutein at site L1 is in contact with Chls that absorb more to the red. On the basis of simple Boltzmann statistics, it is thus expected that more triplets are formed on the Chls in contact with the xanthophyll at site L1, providing an additional explanation why the triplet absorption band at 507 nm is most intense.

Aggregation Leads to a Change in Interaction between Xanthophylls and Chlorophylls. Upon aggregation, the triplet absorption band at 525 nm becomes relatively more intense. It was argued above that this band is due to the lutein at site L2. It should be noted that the total amount of triplet transfer from Chl to Car is independent of the state of aggregation and is ~82% at 5 K as was shown by Barzda et al. (*7*). Therefore, the change in the ratio of the intensities of the 507 and 525 nm triplet bands should be explained by a redistribution of the triplets over the xanthophylls at sites L1 and L2. The redistribution might in principle be due to a change in distribution of the triplets over the different Chls without changing the Chl–Car interactions, i.e., a purely statistical effect due to aggregation-dependent changes in the Chl absorption leading to a change in the Boltzmann distribution of the singlet excitations over the different Chls and concomitantly in the distribution of triplets over the different Chls. Although it was claimed that the absorption spectra of trimers and aggregates are nearly identical and that the difference is entirely due to scattering and sieving effects (*37*), evidence was provided that real changes in the electronic transitions occur (see, e.g., ref *38*) and therefore, such an effect might occur. However, if a redistribution of singlet excitations would occur, one would expect that also the contribution of the 525 nm band in the 2|E| spectrum would concomitantly increase. As can be seen in Figure 2b, such an increase is not observed, and the ratio of the 507 and 525 nm bands remains essentially unaltered. Therefore, it must be concluded that aggregation leads to a change in the interactions between the carotenoids at site L1 and L2 and some of the nearby Chl *a* molecules. It is interesting to note that Ruban et al. observed conformational changes of carotenoids upon oligomerization of LHCII (*39–41*), which may well be related to the change in interaction.

A Possible Explanation for the Aggregation-Induced Shortening of the Singlet Excited-State Lifetime of Chl a in LHCII. It is well-known that aggregation of LHCII leads to a decrease of the singlet excited-state lifetime of Chl *a* in LHCII and a concomitant decrease of the fluorescence quantum yield (see, for instance, refs *42* and *43*). This decrease factor appears to be variable and dependent on preparation, and typical values range from 4 to 6 (*42*, *43*). It was recently argued that a change in the interaction strength between xanthophylls and chlorophylls may cause a change in the excited-state lifetime of Chl, and a simple quantitative relationship was proposed (*27–29*), but a change in interaction upon aggregation has never been reported. In this study, we have presented experimental evidence that the Chl–Car interaction indeed changes upon aggregation of LHCII, and we hypothesize that this change may be responsible for the observed change in lifetime. It should be noted that Razi Naqvi et al. (*8*) observed that the aggregation of LHCII led to a broadening of the TmS spectrum in the xanthophyll region toward the red, in agreement with an increased population of triplets on the xanthophyll at site L2. In parallel, they observed an increased change in the Chl *a* Q_y absorption region. At that time, the change in the spectra were ascribed to increased intertrimer triplet transfer. However, from the present study, it appears that there is a relative increase of triplet transfer to the xanthophyll bound at site L2. Apparently, this leads to a larger change in the absorption of the interacting chlorophylls, suggesting a stronger interaction between the corresponding xanthophyll and neighboring chlorophylls. This is consistent with the proposal that an increase in interaction leads to a decrease in lifetime (*27–29*). Numerous studies have appeared in which the lifetime shortening upon aggregation was studied, and it has been argued that this effect is possibly related to the phenomenon of nonphotochemical quenching (*30*). The latter is an important protective regulatory mechanism, which shortens the lifetime of singlet excitations in photosystem II of green plants, thereby lowering the probability of photoinhibition.

Lampoura et al.

REFERENCES

1. Van Grondelle, R., Dekker, J. P., Gillbro, T., and Sundström, V. (1994) *Biochim. Biophys. Acta 1187*, 1−65.
2. Van Amerongen, H., Valkunas, L., and van Grondelle, R. (2000) Photosynthetic Excitons, World Scientific, Singapore.
3. Sieferman-Harms, D. (1995) *Biochim. Biophys. Acta 811*, 325−335.
4. Carbonera, D., Giacometti, G., Agostini, G., and Toffoletti, A. (1989) *Gazetta Chim. It. 119*, 225−228.
5. Peterman, E. J. G., Dukker, F. M., van Grondelle, R., and van Amerongen, H. (1995) *Biophys. J. 69*, 2670−2678.
6. Peterman, E. J. G., Gradinaru, C. C., Calkoen, F., Borst, J. C., van Grondelle, R., and van Amerongen, H. (1997) *Biochemistry 36*, 12208−12215.
7. Barzda, V., Peterman, E. J. G., van Grondelle, R., and van Amerongen, H. (1998) *Biochemistry 37*, 546−561.
8. Razi Naqvi, K., Melø, T. B., Raju, B., Jávorfi, T., Simidjiev, I., and Garab, G. (1997) *Spectrochim. Acta Part A 53*, 2659−2667.
9. Sieferman-Harms, D., and Angerhofer, A. (1998) *Photosynth. Res. 55*, 83−94.
10. Schödel, R., Irrgang, K. D., Voigt, J., and Renger, G. (1998) *Biophys. J. 75*, 3143−3153.
11. Van der Vos, R., Carbonera, D., and Hoff, A. J. (1991) *Appl. Magn. Res. 2*, 179−202.
12. Van der Vos, R., Franken, E. M., and Hoff, A. J. (1994) *Biochim. Biophys. Acta 1188*, 243−250.
13. Kühlbrandt, W., Wang, D. N., and Fujiyoshi, Y. (1994) *Nature 367*, 614−621.
14. Croce, R., Remelli, R., Varotto, C., Breton, J., and Bassi, R. (1999) *FEBS Lett. 456*, 1−6.
15. Gradinaru, C. C., van Stokkum, I. H. M., van Grondelle, R., and van Amerongen, H. (2000) *J. Phys. Chem. B 104*, 9330−9342.
16. Peterman, E. J. G., Monshouwer, R., van Stokkum, I. H. M., van Grondelle, R., and van Amerongen, H. (1997) *Chem. Phys. Lett. 264*, 279−284.
17. Ruban, A. V., Lee, P. J., Wentworth, M., Young, A. J., and Horton, P. (1999) *J. Biol. Chem. 274*, 10458−10465.
18. Caffarri, C., Croce, R., Breton, J., and Bassi, R. (2001) *J. Biol. Chem. 276*, 35924−35933.
19. Croce, R., Weiss, S., and Bassi, R. (1999) *J. Biol. Chem. 274*, 29613−29623.
20. Gradinaru, C. C., Özdemir, S., Gülen, D., van Stokkum, I. H. M., van Grondelle, R., and van Amerongen, H. (1998) *Biophys. J. 75*, 3064−3077.
21. Barzda, V., Garab, G., Gulbinas, V., and Valkunas, L. (1995) *In Photosynthesis: from Light to Biosphere* (Mathis, P., Ed.) Vol. I, pp 319−322, Kluwer, Dordrecht.
22. Ide, J. P., Klug, D. R., Kühlbrandt, W., Giorgi, L. B., and Porter, G. (1987) *Biochim. Biophys. Acta 893*, 349−364.
23. Simidjiev, I., Barzda, V., Mustardy L., and Garab, G. (1997) *Anal. Biochem. 250*, 169−175.
24. Carbonera, D., and Giacometti, G. (1992) *Rend. Fis. Acc. Lincei 3*, 361−368.
25. Ruban, A. V., Pascal, A. A., and Robert, B. (2000) *FEBS Lett. 477*, 181−185.
26. Ruban, A. V., Pascal, A. A., and Robert, B. (2001) *J. Biol. Chem. 276*, 24862−24870.
27. Van Amerongen, H., and van Grondelle, R. (2001) *J. Phys. Chem. B 105*, 604−617.
28. Razi Naqvi, K., Jávorfi, T., Melo, T. B., and Garab, G. (1999) *Spectrochim. Acta Part A 55*, 193−204.
29. Razi Naqvi, K. (1998) in *Photosynthesis: Mechanism and Effects* (Garab, G., Ed.) Vol. 1, pp 265−270, Kluwer Academic Publishers, Dordrecht.
30. Horton, P., Ruban, A. V., and Walters, R. G. (1996) *Annu. Rev. Plant Physiol. Plant Mol. Biol. 47*, 655−684.
31. Barzda, V., Mustardy, L., and Garab, G. (1994) *Biochemistry 33*, 10837−10841.
32. Van Mourik, F., van der Oord, J. R., Visscher, K. J., Parkes-Loach, P. S., Loach, P. A., Visschers, R. W., and van Grondelle, R. (1991) *Biochim. Biophys. Acta 1059*, 111−119.
33. Van Stokkkum, I. H. M., Scherer, T., Brouwer, A. M., and Verhoeven, J. W. (1994) *J. Phys. Chem. 98*, 852−866.
34. Hobe, S., Niemeier, H., Bender, A., and Paulsen, H. (2000) *Eur. J. Biochem. 267*, 616−624.
35. Bassi, R., and Caffarri, S. (2000) *Photosynth. Res. 64*, 243−256.
36. Remelli, R., Varotto, C., Sandona, D., Croce, R., and Bassi, R. (1999) *J. Biol. Chem. 274*, 33510−33521.
37. Razi Naqvi, K., Melo, B. B., Raju, B. B., Javorfi, T., and Garab, G. (1997) *Spectrochim. Acta Part A 53*, 1925−1936.
38. Ruban, A. V., Calkoen, F., Kwa, S. L. S., van Grondelle, R., Horton, P., and Dekker, J. P. (1997) *Biochim. Biophys. Acta 1321*, 61−70.
39. Ruban, A. V., Horton, P., and Robert, B. (1995) *Biochemistry 34*, 2333−2337.
40. Ruban, A. V., Pascal, A. A., Robert, B., and Horton, P (2001) *J. Biol. Chem. 276*, 24862−24870.
41. Ruban, A. V., Pascal, A. A., and Robert, B. (2000) *FEBS Lett. 477*, 181−185.
42. Barzda, V., Vengris, M., Valkunas, L., van Grondelle, R., and van Amerongen, H. (2000) *Biochemistry 39*, 10468−10477.
43. Barzda, V., Gulbinas, V., Kananavicius, R., van Amerongen, H., van Grondelle, R., and Valkunas, L. (2001) *Biophys. J. 80*, 2409−2421.

BI025724X